Criticality and crossover in accessible regimes

G. Orkoulas, A. Z. Panagiotopoulos, and Michael E. Fisher
Institute for Physical Science and Technology, University of Maryland, College Park, Maryland 20742-2431
(Received 22 October 1999)

The near-critical behavior of $(d=3)$-dimensional Ising-model ferromagnets or simple lattice gases with equivalent first, second, and third nearest-neighbor interactions is studied through Monte Carlo simulations using histogram reweighting techniques and comparisons with series expansions. By carefully analyzing numerical data from relatively small finite systems using scaling and extrapolation methods, it is demonstrated that one can reliably estimate critical exponents, critical temperatures, and universal amplitude ratios, thereby distinguishing convincingly between different ''nearby'' universality classes and revealing systematic crossover effects. This study is preparatory to extending similar techniques to study criticality in continuum fluid models lacking symmetries, with Coulomb interactions, etc.

PACS number(s): 02.70.Lq, 05.50.+g, 05.70.Jk, 64.60.Fr

I. INTRODUCTION

The analysis of near-critical data from Monte Carlo simulations of finite systems has received considerable attention in recent years [1–9]. Given a series of simulations of, say, a model fluid, one is generally interested in elucidating the phase diagram and, in particular, in estimating the location of the critical point and the associated critical exponents. A primary aim then is to identify the appropriate universality class among those that characterize the spectrum of critical behavior; and it may be especially important to clarify the possibilities of crossover between different types of criticality [10–19].

Of notable current interest are *continuum* fluid models suitable for describing real gas-liquid and liquid-liquid critical behavior. While it is widely believed that essentially all such systems should belong to the $(d=3)$-dimensional Ising or, equivalently (in the family of O(n) criticality [20,21]), the $n=1$ universality class, the support for that conclusion from numerical and analytical studies is disappointingly weak amounting, typically, to not much more than the demonstration of plausibility or consistency [8,22–27]. This fact has been especially highlighted in the last few years by the experimental [28–32] and theoretical quest [24–26,33–38] to understand and characterize the nature of criticality in real 1:1 electrolytes or, theoretically, in the most basic, nonquantal ionic or Coulomb system, namely, the so-called ''restricted primitive model.'' Among the disparate views that have been advanced are that ionic criticality should be of classical, i.e., mean-field or van der Waals nature (corresponding to $d>4$, $n=1$), *or*, by contrast, of Ising type, *or* should display crossover from classical to $d=3$ Ising behavior with a crossover temperature (close to T_c) characterized in some way by particular microscopic properties of the systems in question [36–38]. The possibility of tricritical or near-tricritical behavior has also been raised [34,35,37].

Similar issues arise in studying phase transitions in more complex systems such as 2:1 electrolytes, colloids [39], polymer solutions (where crossover on approach to the θ point has been clearly identified experimentally [19]), dipolar and ferrofluids, network-forming and micellar systems.

The major difficulties in attacking the problem of criticality in continuum fluids by numerical simulations are (a) the strongly limited accessible system sizes (measured, say, by the linear dimension L expressed in units of the microscopic repulsive core diameter a) constrained both (i) by the difficulties of reliably sampling equilibrium distributions, owing to critical slowing down, and (ii) the needs of storage and speed in handling configurations and computing energies, etc., especially when long-range forces act; (b) the absence, in realistic models, of special symmetries, such as displayed by simple lattice gases, and the consequent need to study, say, the two-parameter density temperature or (ρ,T) plane and then estimate *both* ρ_c and T_c, rather than simply tracking a single critical locus; and, finally, (c) the fact, again arising from lack of symmetry, that the expected asymptotic thermodynamic scaling properties are both more complex and less well understood for fluid systems than for lattice-based models. (It might be remarked that points (a ii), (b), and (c) equally hamper series expansion techniques [40–43].)

By contrast, for lattice models one can attain much greater relative system sizes L than in continuum systems, and so approach more closely bulk asymptotic critical behavior. This is so, in part, (i) because effective algorithms for ameliorating critical slowing down are available [44,45] and (ii) because the demands for storing configurations and computing energies, etc., are significantly diminished. The greater range of L accessible computationally permits the effective use of *finite-size scaling techniques* [2,4,5,46,47] to extrapolate reliably to the thermodynamic limit, $L\to\infty$. Thus recent impressive, large-scale studies [12–16] have convincingly demonstrated crossover in a lattice gas from Ising to classical behavior as the range of interaction R_0 becomes infinite (relative to the single-site hard-core diameter or lattice spacing a). Even the anticipated universal nature of the asymptotic crossover, specifically as seen in the *effective, range-dependent critical exponents*, has proven amenable to study [16].

To match such an achievement in a continuum model lacking a strong symmetry is surely beyond current (or even foreseeable) possibilities. Nevertheless, we believe that by an extended, more systematic, and theoretically well-informed study of the finite-size variation of near-critical properties,

even with only a limited range of sizes, L, significant further progress in understanding criticality in continuum systems can be made. This paper represents a first step on the path to that goal. Our aim here is to test a range of finite-size scaling techniques on a ''modestly complex,'' but relatively well-understood problem, *without* great expenditure of computational effort.

To that end we have chosen to examine the simple-cubic (sc) lattice gas with equivalent first, first-plus-second, and first-plus-second-plus-third neighbor interactions (and ''trivial'' single-site hard cores)—in effect, Ising ferromagnets with coordination numbers $q=6$ (the standard sc model), $q=18$, and $q=26$ [48–50]. One can be highly confident that this model belongs to the Ising universality class for all $q<\infty$ [10,20,51]; but our question is: With what degree of precision and conviction can this conclusion actually be demonstrated using simulations running up to sizes $L/a=10$ to 20? In fact, one knows [10,51–53] that when $q\to\infty$ (so that $R_0\to\infty$) the critical behavior becomes classical and is described precisely by standard mean-field theory [53]. Furthermore, signs of this crossover are clearly visible, and must be dealt with, even for q as small as 18 and 26. Indeed, an ancillary aim of our study is to exhibit the appearance of these crossover effects outside the immediate critical neighborhood [the latter defined, say, by $t=(T-T_c)/T_c \lesssim 0.03$], since we anticipate that closely related behavior will be observed in continuum models, such as Lennard-Jones systems and the hard-core square-well fluid [22,23,26], for which system we plan to report detailed results in the future.

Our investigations comprise a series of Monte Carlo simulations for sizes $L/a\geqslant 6$ [54]. The data have been handled by histogram reweighting techniques [55] that provide requisite flexibility for detailed analysis. The information obtained with the aid of finite-size scaling methods confirms that the approach to criticality is governed by Ising exponents to an apparent precision that excludes the numerically closest, well-known, $d=3$ universality classes, namely, $n=0$, describing self-avoiding walks or polymers, and $n=2$ as appropriate for *XY* or ''easy plane'' ferromagnets, and superfluids [20,56]. Van der Waals, mean-field exponents lie well outside this range. Having obtained a reasonable estimate of the critical temperatures T_c, a miscellany of quantities, such as effective exponents and dimensionless amplitude ratios, can also be computed. Comparisons with series expansion data [48–50] (inevitably limited in length for $q\geqslant 18$) have also been made: The Monte Carlo data for $q=18$ and 26 prove fully competitive near criticality if not actually superior. One can thus, indeed, obtain a very adequate description of the near-critical description of a ''modestly complex'' lattice fluid from numerical simulations involving systems of moderate size. We may thus hope that similar methods, but necessarily developed to allow for lack of gas-liquid symmetry, will yield comparable results for at least the simpler continuum fluids.

II. MODEL SYSTEMS AND METHODOLOGIES

The well-known Ising model comprises spins $s_j=\pm 1$, located at the sites j of a d-dimensional lattice of linear dimension L. For ferromagnetic systems, which are of interest in this work, the interaction energy between a pair of coupled spins is given by $-Js_is_j$, where $J>0$ is the strength of the interaction. The interaction between a spin s_j and the externally imposed magnetic field, H, is $-Hs_j$. Upon defining a reduced coupling strength and a reduced magnetic field via

$$K=J/k_BT,\quad h=H/k_BT, \tag{1}$$

respectively, the partition function can be written as

$$Z(k,h)=\mathrm{Tr}[\exp(-KE+hM)], \tag{2}$$

where the reduced energy, defined by

$$E=-\sum_{\langle ij\rangle} s_is_j, \tag{3}$$

includes interactions between all coupled pairs $\langle ij\rangle$, and the magnetization is

$$M=\sum_j s_j. \tag{4}$$

We will specifically consider the $(d=3)$-dimensional simple cubic (sc) lattice with equal ''equivalent neighbor interactions'' reaching out to the first, second, and third coordination shells and so encompassing $q=6$, 18, and 26 neighbors.

Histogram reweighting techniques [55] allow one to greatly enhance the information that can be obtained from a single simulation run. According to these procedures, one performs a simulation at a state point (K_0,h_0) and stores the instantaneous values of the energy, E, and magnetization, M, in the form of a histogram $f_0(E,M)$. The histogram $f(E,M;K,h)$ for a state (K,h), not too far away from (K_0,h_0), can be obtained from $f_0(E,M)$ via the simple rescaling

$$\frac{f(E,M;K,h)}{f_0(E,M)}\propto\exp[-(K-K_0)E+(h-h_0)M], \tag{5}$$

without the need to perform any additional simulations. Properties of interest, such as heat capacities, susceptibilities, etc. can subsequently be obtained in terms of weighted sums or moments of the appropriate histogram, e.g.,

$$\langle X\rangle_{K,h}=\frac{\sum_{E,M} X(E,M)f(E,M;K,h)}{\sum_{E,M} f(E,M;K,h)}. \tag{6}$$

Near a critical point properties exhibit finite-size rounding since the growth of the correlation length is limited by the linear dimensions of the finite system. Finite-size scaling theory [46,47], a generalization of the original thermodynamic scaling concept, is designed to describe the rounding and shifting effects invariably observed in finite systems. Specifically, a property $Y(T)$ (assuming for simplicity $h=0$) that exhibits a power-law type of divergence in the thermodynamic limit so that

$$Y(T)\sim|t|^{-\omega},\quad t=(T-T_c)/T_c, \tag{7}$$

is, in general, expected to scale as

$$Y(T) \approx L^{\omega/\nu} \tilde{Y}(tL^{1/\nu}) \tag{8}$$

in the limit of large L. Here, ν is the universal correlation length exponent for the class of systems in question and $\tilde{Y}$ is a universal scaling function. Of course, various further corrections will inevitably show up for small sizes. The scaling form (8) typically implies that a diverging quantity will reach a maximum value of height proportional to $L^{\omega/\nu}$. Moreover, the location of the maximum, which may be regarded as an effective critical point, say, $T_c^{(Y)}(L)$, should vary with the system size as

$$T_c^{(Y)}(L) - T_c(\infty) \sim L^{-1/\nu}. \tag{9}$$

In attempting to determine the infinite-volume critical temperature using numerical data gained from finite systems, one often determines the peak positions of the second and higher order derivatives of the free energy for a series of increasing values of L and subsequently extrapolates to the thermodynamic limit according to (9). However, to do this effectively, the appropriate correlation length exponent ν must be found (or ''known'') prior to the extrapolation.

There have been numerous studies that aim to estimate critical point exponents from numerical data for finite systems [57]. Early approaches, with relatively limited data, utilized the full scaling form (8). Specifically, one represents the data in terms of scaled variables by, say, plotting $Y/L^{\omega/\nu}$ vs $tL^{1/\nu}$, and then adjusts the values of both the exponents and the critical temperature so that a satisfactory data collapse is attained. In practice, however, this method suffers not only from random sampling errors but, more importantly, from systematic errors. Experience shows that excellent data collapse can frequently be obtained with significantly erroneous exponents. Indeed, as emphasized by Binder [3,9], Eq. (8) is an asymptotic expression that is accurate only in the limit of large L: it does not allow for the various correction terms pertaining to small L so that fitting to Eq. (8) inexorably leads to systematic errors unless L is very large. Inclusion of additional correction terms leads to many-parameter nonlinear fits with, in general, unavoidable instabilities and strongly coupled uncertainties.

A somewhat different procedure is based on the behavior of the so-called Binder cumulant [58] along the symmetry axis ($h=0$). This parameter is defined by

$$U_L \equiv Y_0(T) = 1 - \tfrac{1}{3} \langle M^4 \rangle / \langle M^2 \rangle^2 \tag{10}$$

and approaches well-defined and distinct limits for $T \gg T_c$ and $T \ll T_c$, respectively. Owing to the absence of an L-dependent factor in the appropriate scaling form for U_L [in contrast to Eq. (8)], the cumulant is expected to attain a universal value at $T = T_c$. Plotting U_L against T for a series of values of L is thus expected to reveal a common intersection point, which then provides an estimate of T_c. However, due to the inextricable presence of correction terms associated with small L, one usually observes a series of somewhat scattered points instead of a unique intersection: the value of T_c so determined will then not be very precise. An estimate of ν may, nevertheless, be obtained by analyzing the cumulant slopes around the intersection points.

Along these lines, one may invent numerous exponent estimators; but they all appear to be biased in that they are based on some prior knowledge of T_c. Consequently, in the present work, we have adopted a rather different route that assumes there is a unique T_c but does not require prior knowledge concerning its value. To this end, consider the peak positions, say $T_j(L)$ and $T_k(L)$, for a pair of properties $Y_j(T)$ and $Y_k(T)$, respectively. By (9) one can write

$$T_i(L) = T_c + Q_i L^{-1/\nu} + \cdots, \tag{11}$$

for $i=j$ and k. Then by eliminating the true but unknown infinite-volume critical temperature T_c, one obtains

$$\Delta T_{jk}(L) = T_j(L) - T_k(L) \approx (Q_j - Q_k) L^{-1/\nu}. \tag{12}$$

At this stage, an estimate of ν independent of T_c can be obtained by, say, considering two distinct linear sizes L_1 and L_2 and studying the ratio

$$R_{jk} = \frac{\Delta T_{jk}(L_2)}{\Delta T_{jk}(L_1)} \approx \left(\frac{L_1}{L_2} \right)^{1/\nu}. \tag{13}$$

An explicit implementation of this approach, employing a fixed increment, $L_2 - L_1 = \Delta L$, and extrapolation on L_1, is explained below and illustrated in Fig. 1.

III. RESULTS AND DISCUSSION

As indicated, we have performed Monte Carlo simulations for ferromagnetic Ising models with up to first ($q=6$), second ($q=18$), and third ($q=26$) neighbor interactions and for linear sizes L from 6 to 20 lattice spacings. All simulations were performed in zero field ($h=0$). The total length of each simulation was in the range of $(5-20)\times 10^6$ trial spin flips per lattice site depending on the system size. (We remark, parenthetically, that we opted to use the traditional, unsophisticated Metropolis algorithm [54], rather than program appropriate cluster algorithms [44,45], since, on the one hand, the former is more readily transferable to nonsymmetric and off-lattice situations and, on the other hand, we were not aiming for maximal precision and accuracy or very large system sizes.) The primary output of our simulations comprised the joint distribution of magnetization and energy, $f(E,M)$, in the form of two-dimensional histograms with bins of size $\Delta M = 2$ and $\Delta E = 4k$ (where $k \geqslant 1$ is a small integer) in accord with (3), (4), and $s_j = \pm 1$.

The raw data were analyzed through histogram reweighting and the derivatives of the free energy were subsequently calculated for a large number of near-critical states. Such derivatives can be expressed in terms of the magnetization and energy moments, $\langle |M|^n \rangle$ and $\langle E^m \rangle$, and the cross moments $\langle E^m |M|^n \rangle$. From these we also calculated (for $h=0$) the Binder cumulant $Y_0 \equiv U_L$, as defined in (10), its temperature derivative, $Y_1 \equiv (dU_L/dT)_{h=0}$, which has a sharp negative peak, thereby defining the estimator $T_1(L)$, and the reduced heat capacity density

$$C \equiv Y_2(T) = L^{-d} K^2 [\langle E^2 \rangle - \langle E \rangle^2], \tag{14}$$

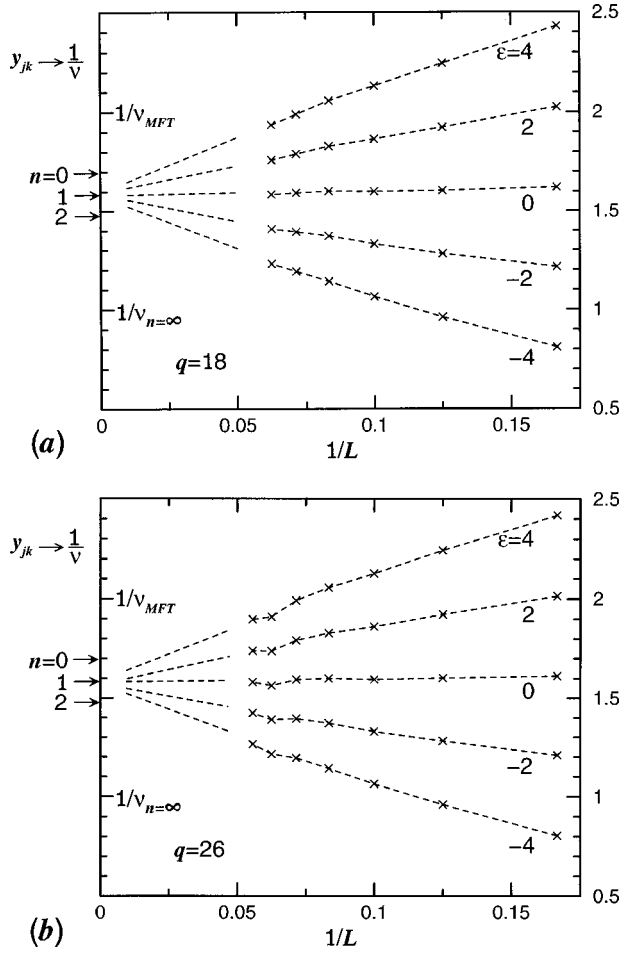

FIG. 1. Illustration of the estimation of the inverse correlation length exponent $1/\nu$ for the Ising model (a) with $q=18$ and (b) with $q=26$ equivalent neighbors using the estimators y_{jk} defined in (19). In this and further figures L is measured in units of the lattice spacing a. The pairs of moment-derived properties used here are $Y_3 \equiv \check{\chi}_2$ (see text) and $Y_4 \equiv L^{-d}(d\langle|M|\rangle/dT)_{h=0}$. Examination of other combinations of the Y_j mentioned in the text leads to similar conclusions. The adjustable shift parameter ε allows for additional finite-size corrections; see (19). The arrows on the ordinate indicate, from the highest downwards, favored estimates of $1/\nu$ for $n=0$ (self-avoiding walks), $n=1$ (Ising), and $n=2$ (XY) systems [20,56]. The values $1/\nu=2$ and 1 correspond to mean-field theory and the spherical model ($n=\infty$) [10,20,21], respectively.

which peaks at $T_2(L)$. It is convenient here and below to measure L in units of the lattice spacing a: thus $k_B C(T)$ is the heat capacity per lattice site.

The behavior of the finite-size susceptibility $\chi_2 = L^{-d}\langle M^2\rangle$ ($h=0$) is also of interest; but since this does *not* display an extremum in the critical region, we have also examined the *modified* or *connected susceptibility*

$$\check{\chi}_2 \equiv Y_3(T) = L^{-d}[\langle M^2\rangle - \langle|M|\rangle^2], \tag{15}$$

in which the first moment of the magnetization *magnitude* $|M|$ has been introduced. Recall that $\langle M\rangle_L \equiv 0$ when $h=0$ for T above or below T_c. For finite L this function has a sharp maximum at $T_3(L)$. However, in the limit $L\to\infty$ we expect that $\check{\chi}_2(L;T,h=0)$ will approach the ''zero-field'' susceptibility

$$\chi_2(T,h=0) \equiv \lim_{h\to 0^+} \lim_{L\to\infty} L^{-d}(\partial\langle M\rangle_{L,T,h}/\partial h), \tag{16}$$

where the order of limits must be respected.

For similar reasons, we have also examined $Y_4(T) \equiv L^{-d}(d\langle|M|\rangle/dT)_{h=0}$ and

$$\check{\chi}_3 \equiv Y_5(T) = L^{-d}[\langle|M|^3\rangle - 3\langle|M|\rangle\langle M^2\rangle + 2\langle|M|\rangle^3], \tag{17}$$

and the fourth order analog

$$\check{\chi}_4 \equiv Y_6(T) = L^{-d}[\langle M^4\rangle - 4\langle|M|\rangle\langle|M|^3\rangle + 12\langle M^2\rangle\langle|M|\rangle^2 - 3\langle M^2\rangle^2 - 6\langle|M|\rangle^4]. \tag{18}$$

These quantities exhibit two finite-size extrema $T_5^{\pm}$ and $T_6^{\pm}$, which approach T_c from above $(+)$ and below $(-)$, respectively.

The next task involves the analysis of the peak locations $T_j(L)$ in order to estimate ν. We did not attempt to use (13) directly since the accessible sizes are relatively small and significant deviations from asymptotic scaling are thus expected. Such deviations manifest themselves as corrections to asymptotic power laws (often called ''corrections to scaling''), corrections to the finite-size scaling forms (8), and corrections due to nonlinearities in the scaling ''fields'' [i.e., the variables entering (8)]. Accordingly, we have linearized (13) for pairs of system sizes $L_1=L$ and $L_2=L+\Delta L$ and then obtain

$$y_{jk} \equiv (1-R_{jk})\frac{(L+\varepsilon)}{\Delta L} \to \frac{1}{\nu} \text{ as } L\to\infty, \tag{19}$$

where the adjustable small, fixed ''shift'' parameter ε has been introduced to provide some account of higher order L-dependent corrections; notice that $(L+\varepsilon)^{-1} = L^{-1}(1 - \varepsilon L^{-1} + \cdots)$. The use of such a shift parameter is well established in series extrapolation studies (see, e.g., [42]). Its primary role is to yield a set of different sequences converging to the limit at different rates and from various directions; see Fig. 1. In that way one is less likely to be led astray by some ''accidentally good'' (apparently) simple behavior. Beyond that, one should be aware that in exactly soluble finite-size lattice critical problems, one typically finds the appearance of factors $(L+\frac{1}{2})$, $(L-\frac{1}{2})$, $(L+1)$, etc. To this degree, then, the appearance of ε can be regarded as analogous to an ''analytical background'' term as present, say, in a bulk specific heat $C_V(T)$ that diverges at criticality. If one is convinced *a priori* that the critical behavior is of Ising type, one might well hope to see a leading correction-to-scaling term of the form $L^{-\theta/\nu}$ with $\theta/\nu \simeq 0.83$, rather than merely L^{-1} as one could regard the implication of including ε as in (19). The dominance of such a correction term will result, asymptotically as $L\to\infty$, in a ''blunting'' of the ''arrowhead'' formed by a set of plots for different ε (see Fig. 1). To the extent that this is not observed in the data the singular correction term might be judged absent. That, however, would be a mistake. As indicated, an ε-type correction should always be present and, numerically, a $1/L$ term will be difficult to resolve from a $1/L^{0.83}$ term (and from other terms with exponents not greatly exceeding unity). This is especially true for the relatively small values of L accessible in these

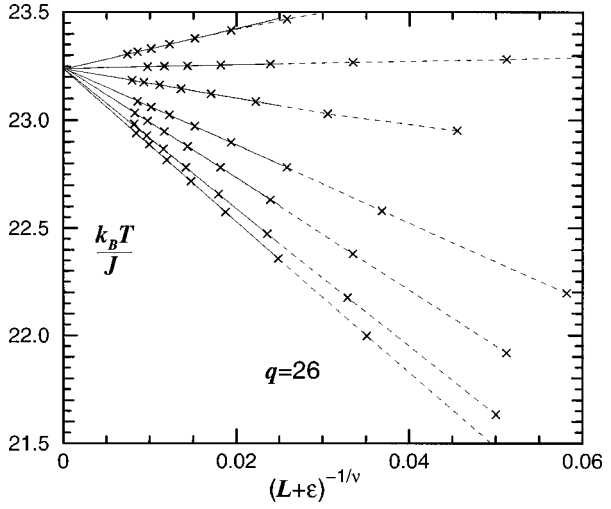

FIG. 2. Critical temperature estimation for the Ising model with $q=26$ equivalent neighbors by extrapolation to infinite size ($L\to\infty$) using a variety of moment criteria. A value of $\nu=0.630$ is assumed. The adjustable shift parameter ε is incorporated to partially compensate for the higher order finite-size scaling corrections. The plots, from the highest downwards, correspond to the properties Y_j for $j=1$ ($\varepsilon=2$), $j=6^{(+)}$ ($\varepsilon=-\frac{3}{2}$), $j=3$ ($\varepsilon=1$), $j=4$ ($\varepsilon=0$), $j=5^{(-)}$ ($\varepsilon=\frac{1}{2}$), $j=2$ ($\varepsilon=0.6$), and $j=6^{(-)}$ ($\varepsilon=\frac{1}{4}$).

(and typical continuum) studies. Thus the use of ε must be regarded, essentially, as an aid to intelligent extrapolation: its ''optimal'' value serves only as an indication of the magnitude of the totality of corrections.

In Fig. 1 we illustrate plots of y_{jk} vs $1/L$ for the sc Ising models with $q=18$ and $q=26$ neighbor couplings. The latter represents the most challenging case since it is known that mean-field (or classical van der Waals) behavior is attained when $1/q\to 0$ [51–53]. In the limit of large L the data appear to extrapolate close to the expected Ising value $\nu\simeq 0.63_0$ [56]. Examination of the plots for the $q=6$ case and for other pairs of properties, Y_j and Y_k, leads to similar conclusions. Thus from Fig. 1(b) we would conclude $\nu=0.63\pm 0.02$, which distinguishes the $q=26$ system well from self-avoiding walks with $\nu\approx 0.58_8$ and *XY*-spin systems with $\nu\approx 0.67_6$ [56].

Having demonstrated that the systems under consideration exhibit Ising behavior, at least as far as the value of ν is concerned, we may proceed to estimate the critical temperature by extrapolating the peak positions $T_j(L)$ in accord with (9). A composite plot vs $1/(L+\varepsilon)^{1/\nu}$ for the $q=26$ model is presented in Fig. 2. It is clear that linear extrapolation allows one to convincingly estimate the critical temperature.

Table I presents our ''moderate-size'' estimates of $1/K_c=k_BT_c/J$ for the three cases $q=6$, 18, and 26 (using $L\leqslant 16$, $\leqslant 20$, $\leqslant 20$, respectively) and compares with estimates already in the literature. The agreement with the reliably known precise value for the standard sc Ising model ($q=6$) [59] is encouraging. Our estimates also agree unexpectedly well with the values recently obtained by Luijten [14] in his large scale study. However, the agreement with the original estimates of Domb and Dalton based on series expansions at high temperatures [49] is relatively poor. This can be attributed to the short length of the series they obtained—one could do somewhat better with current computing power but a significant effort would be required. In addition, Domb and Dalton assumed an Ising value $\gamma=1.250$, known now to be significantly too high (by about 0.010 to 0.013). The last column shows simple Padé estimates using $\gamma=1.239$ (see the Appendix). These are closer to the Monte Carlo estimates but still differ significantly. However, the methods of series analysis used were comparatively unsophisticated since they did not allow for singular corrections to scaling that are almost certainly significant for $q\gtrsim 26$. At this point, then, even our moderate-size estimates for T_c must be judged appreciably more reliable.

Granted reliable estimates of $T_c(\infty)$, other quantities may be studied to confirm (or otherwise) the assignment of universality class. Valuable properties include effective exponents *and* dimensionless amplitude ratios. These allow one not only to characterize the critical behavior with greater certainty but also, and significantly, permit exploration of plausible crossover possibilities. The effective coexistence curve and susceptibility exponents are defined via logarithmic derivatives with respect to the temperature distance from the critical point as measured by

$$t'\equiv t/(1+t)=1-T_c/T=1-K/K_c, \tag{20}$$

TABLE I. Comparison of estimates for the reduced critical temperatures $T_c^*=k_BT_c/J=K_c^{-1}$ for sc Ising models with q equivalent near-neighbor interactions. The uncertainties quoted refer to the last decimal place.

	Monte Carlo simulation		Series expansions[b]	
q	This work	Luijten[a]	$\gamma=1.250$[c]	$\gamma=1.239$[d]
6	4.511 ± 2	$4.511\,52\pm 2$[e]	4.5108[f]	4.512 08[f]
18	15.523 ± 5	$15.522\,57\pm 12$	15.5039	15.51
26	23.235 ± 10	$23.235\,2\pm 2$	23.1481	23.18

[a]See Ref. [14], which employed nonlinear fits to a modified Binder cumulant.
[b]Series for $q=18$ and 26 from Domb and Dalton [49].
[c]Ratio analysis [49] using the estimate $\gamma=1.250$. See also the Padé analysis of Dalton and Wood [50] yielding closely similar results.
[d]Padé analysis assuming $\gamma=1.239$. See the Appendix for $q=18$ and 26.
[e]This value agrees well, up to uncertainties in the last decimal place, with estimates from large-scale simulations utilizing multispin flips, etc. [4,6].
[f]See Liu and Fisher [59]. The values quoted there have been interpolated for the assigned value $\gamma=1.239$.

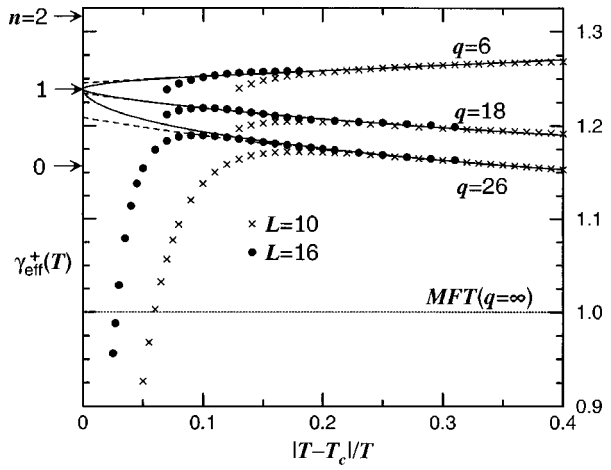

FIG. 3. Effective susceptibility exponent $\gamma^{+}_{\rm eff}(T)$ for $T>T_c$ for sc Ising models with $q=6$, 18, and 26 nearest-neighbor couplings. The points correspond to data obtained from Monte Carlo simulations according to the procedure explained in the text: ×, $L=10$; ●, $L=16$. The arrows indicate the limits for the $n=0$, 1, and 2 universality classes in order of increasing magnitude. The dotted line represents the mean-field theory (or $q=\infty$) result. The solid and dashed curves correspond to Padé approximants constructed from the series expansion data of Domb and co-workers [48–50]; see text and Appendix. Note that in order to avoid confusing the plot, the data for the full finite-size crossover that must take place in all cases when $t'\to 0$ have been shown only for $q=26$. However, the sharpness of the breakaway *and* its shift with increasing L, enables one to extrapolate to large L with reasonable precision down to, say, $t'\simeq 0.02$.

according to the $h=0$ relations

$$\beta_{\rm eff}(T)=\partial \ln\langle|M|\rangle/\partial \ln|t'|, \tag{21}$$

$$\gamma^{\pm}_{\rm eff}(T)=-\partial \ln \chi_2^{\pm}/\partial \ln|t'| \quad (t'\gtrless 0), \tag{22}$$

where $\chi_2^{+}\equiv\chi_2(L;T>T_c,h=0)$ while χ_2^{-} denotes $\check{\chi}_2(L;T<T_c)$ as defined in (15): see also (16).

In Figs. 3, 4, and 5 we present results for $\gamma^{+}_{\rm eff}$, $\gamma^{-}_{\rm eff}$, and $\beta_{\rm eff}$. To obtain these, we performed extra simulations for L

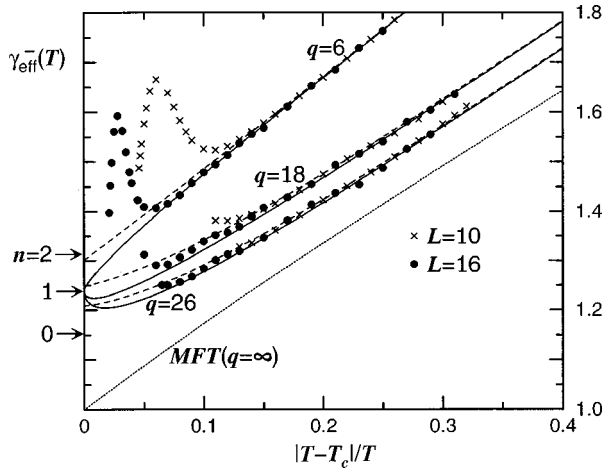

FIG. 4. Effective susceptibility exponent $\gamma^{-}_{\rm eff}(T)$ for $T<T_c$ for sc Ising models with $q=6$, 18, and 26 equivalent neighbor interactions. Lines and points, etc., have the same meaning as in Fig. 3.

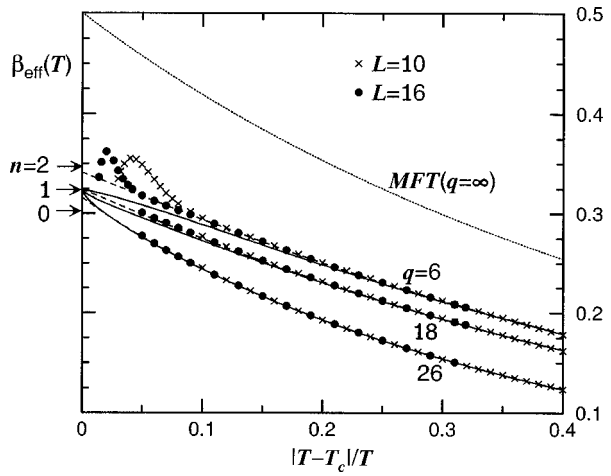

FIG. 5. Coexistence curve exponent $\beta_{\rm eff}(T)$ for sc Ising models with $q=6$, 18, and 26 nearest-neighbor couplings. Lines and points, etc., have the same meaning as in Figs. 3 and 4.

$=10$ and $L=16$ that extended further towards low and high temperatures. These simulations in no way penetrate the asymptotic critical region and finite-size rounding is fully evident. Nevertheless, as $T\to T_c$ the departures from what should be good approximations to the limiting bulk behavior away from T_c are rather sharp; and, as L increases, the ''breakoff'' points quite rapidly approach T_c (in leading order, of course, as $1/L^{1/\nu}$ with $1/\nu\simeq 1.59$). Consequently, one can extrapolate the bulk behavior in towards T_c with reasonable confidence. The values of β and γ so estimated are consistent with the expected Ising values and, taken together, certainly serve to distinguish the appropriate universality class from the $n=0$ (self-avoiding walks) or $n=2$ (XY) classes (even though the data below T_c for $\gamma^{-}_{\rm eff}(T)$ are noisier and less decisive on their own).

One notices, in particular, that for the standard ($q=6$) sc Ising model $\gamma^{+}_{\rm eff}(T)$ approaches $\gamma_{n=1}\simeq 1.23_9$ from *above* as emphasized by Liu and Fisher [60]. [The same will be observed for the nearest-neighbor bcc ($q=8$) and fcc ($q=12$) Ising lattices [60].] On the other hand, on extending the interaction range the effective susceptibility exponent is seen to approach its limiting value from *below*, strongly suggesting that the amplitude of the first correction-to-scaling term in $\gamma^{+}_{\rm eff}(T)$ (in the true asymptotic behavior) changes sign and, in fact, becomes *negative* as the range of interaction increases even by a relatively small factor [14,15]. Such a change is to be expected on intuitive grounds, since, in the limit of very large q, the effective exponent must approach $\gamma_{n=1}$ from a value close to $\gamma_{\rm MFT}=1<\gamma_{n=1}$ [52,53].

It is also evident from Figs. 3–5 that the full crossover between classical and Ising near-critical behavior has not been observed in this work since the values of q studied are relatively small, so that the finite systems leave the critical region before such a crossover can be completed. It is quite striking, nonetheless, that the effective exponents below T_c for $|t|\gtrsim 0.05$ have crossed over by 30 to 40 % of the total magnitude already by $q=26$. The full $d=3$ asymptotic crossover phenomenon, however, has been observed only in the recent Monte Carlo work of Luijten and co-workers [12–16] (who also examined crossover in $d=2$ Ising models with extended interaction ranges).

It may be worth commenting that the variable t' used in Fig. 3 approaches unity when $T\to\infty$. In that limit the effective exponents $\gamma^+_{\rm eff}(T)$ approach limits $\gamma^+_\infty \simeq 1.33$, $\simeq 1.16$, $\simeq 1.12$, for $q=6$, 18, 26, respectively. Crossover to the classical value $\gamma=1$ is not seen; nor should it be expected.

To obtain further insight and, incidentally, as a crosscheck of the simulations away from T_c, we have also constructed various Padé approximants using the available series expansion data of Domb and co-workers [48–50]. Details are presented in the Appendix. The dashed curves in Figs. 3–5 represent simple approximants for the effective exponents (biased only by the value of T_c). The agreement with the ''converged'' simulation results outside the roundoff region is excellent. These plots also approach values at T_c consistent with Ising exponents to quite reasonable accuracy. (Note that for $q=6$ only, series of restricted length [42] have been used.) By contrast the solid plots in the figures have been constructed by imposing favored Ising estimates (namely $\beta \simeq 0.325$, $\gamma \simeq 1.239$ [56,59]) and allowing explicitly for singular correction-to-scaling factors of the form $(1+g|t|^\theta +\cdots)$ with θ taken as 0.54 [61] (but see also [56]); see the Appendix. These plots, which are *not* to be accepted as numerically reliable, serve to give a plausible idea of how the crossover in the effective exponents should appear in the thermodynamic limit ($L\to\infty$).

The information that can be obtained by histogram reweighting is by no means limited to effective exponents. Indeed, dimensionless amplitude ratios constitute examples of quantities that have received relatively little attention in the past but are valuable because they are expected to approach universal limits [59,62–65]. The most accessible of these, namely the critical susceptibility amplitude ratio, which may be defined by

$$\frac{C^+}{C^-} = \lim_{T\to T_c} \mathcal{R}_\chi(T) \quad \text{with} \quad \mathcal{R}_\chi(T) = \frac{\chi_2^+(t')}{\chi_2^-(-t')} \qquad (23)$$

is a strong indicator of universality class. Thus series expansion evidence, renormalization group calculations, and simulations [59,62–65] indicate that the susceptibility ratio takes a universal value of $C^+/C^- \simeq 4.9_5$ in a $d=3$ Ising ($n=1$) system. This is to be contrasted with a classical mean-field value of $C^+/C^-=2$ [59,62,63] and a $d=2$ Ising value of $37.69\ldots$; but note that the ratio is not defined for $d\leqslant 4$ when $n\neq 1$.

Our simulation data for the susceptibility ratio $\mathcal{R}_\chi(T)$ are shown in Fig. 6 together with simple Padé extrapolations: see the Appendix. Both are quite consistent with Ising behavior but certainly inconsistent with the possibility of mean-field character. Note, however, that for $q=26$ and $|t| \gtrsim 0.05$ the effective crossover to the mean-field limit from the nearest-neighbor behavior is over 40% complete. Nevertheless, much larger simulations [14] or much longer series would be needed to uncover the full crossover for greater values of q.

Another critical amplitude ratio of particular theoretical significance is A^+/A^-, for the specific heats above and below T_c. This is closely correlated with the value of the specific heat exponent $\alpha \simeq 0.10_9$ (for $n=1$) since, rather generally, $A^+/A^-=1$ for $\alpha=0$(log). However, the specific heat is weakly divergent with a relatively small amplitude and a large, rapidly varying background contribution through T_c [59]. Furthermore, in a finite periodic system it displays a large shift $T_c(\infty)-T_c(L)>0$. For these reasons, the current simulations are too small in size to examine an analog of Fig. 6. Moreover, as illustrated in Fig. 7, quite marked changes in form arise as q increases. By plotting against the temperature

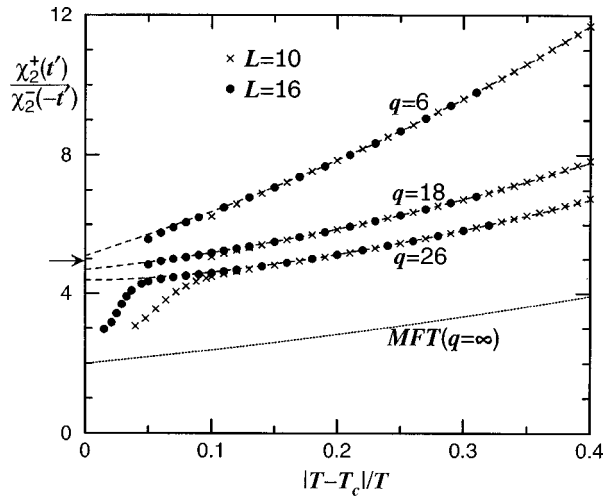

FIG. 6. Susceptibility amplitude ratio $\mathcal{R}_\chi(T)=\chi_2^+(t')/\chi_2^-(-t')$ for Ising models with $q=6$, 18, and 26 nearest-neighbor couplings. The arrow indicates the expected universal critical point ratio for $d=3$ Ising-type systems. The dashed curves derive from simple Padé approximants: see the Appendix.

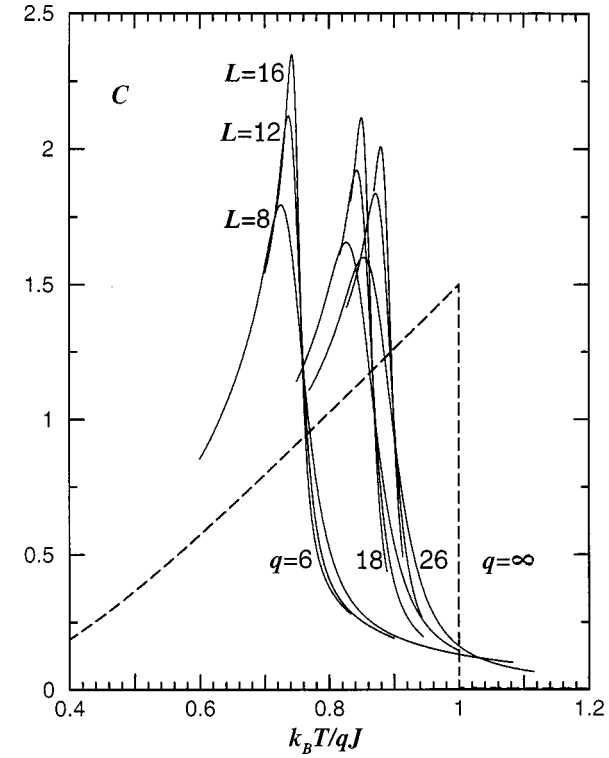

FIG. 7. Reduced heat capacity per site for sc Ising models with $q=6$, 18, and 26 equivalent neighbor couplings and system sizes $L=8$, 12, and 16 plotted vs $T^\uparrow=k_BT/qJ$. The bulk mean-field heat capacity, which is approached when $q\to\infty$, is shown as a dashed curve; it vanishes identically above T_c.

scaled by a factor q, the crossover to the limiting mean-field behavior is revealed at least qualitatively. (It is also interesting to compare with Fig. 7 of Liu and Fisher [59] which presents the bulk specific heats for the nearest-neighbor sc, bcc, and fcc Ising lattices with coordination numbers $q=6$, 8, and 12, respectively.)

IV. CONCLUSIONS

We have shown that Monte Carlo simulations of ''moderately complex'' lattice systems of relatively small size, in which the critical point is strongly rounded, can through careful, flexible, and systematic finite-size analyses provide reliable, unambiguous, and fairly precise characterization of their critical behavior. The essence of our method, taking advantage of histogram reweighting, is to examine the rounding and convergence behavior of a variety of distinct ''critical-point indicators'' through the whole critical region on approach from *all* directions: in the present, symmetric examples that merely means from *above* T_c as well as from *below*. While recognizing fully that *any* fixed numerical technique will always be defeated by a sufficiently subtle or complex problem, we believe our comparative success on these ''moderately complex'' examples provides grounds for optimism that a similar approach will yield significant gains over previous treatments for nonsymmetric and off-lattice or continuum systems. Primary candidates for study are hard-core square-well fluids [22,23,26]: Ising-type critical behavior can certainly be expected; but the task is to demonstrate that unambiguously and precisely. One needs, furthermore, to discover how to deal more effectively with the lack of symmetry inherent in such models and thereby to reveal fully the concomitant mixing of scaling fields and the associated implications. It is clear from the present study that a systematic attack, in such cases, must not only study the approach to the critical region from above and below in temperature as a function of system size but *also*, and crucially, as a function of chemical potential and density as the size changes. Again, it is evident that the information contained in the fluctuations in density and energy can provide primary insight beyond that gained in the recent focus on the effective coexistence curve and its evolution with system size [7,8]. In fact, such work is underway and will be reported in due course. The task of definitively clarifying the issue of ionic criticality in model electrolytes may then be attacked afresh.

ACKNOWLEDGMENTS

We appreciate the interest of Professor J. V. Sengers and Professor M. A. Anisimov. The support of the National Science Foundation (through Grant No. CHE 96-14495 to M.E.F.) and of the Department of Energy, Office of Basic Energy Sciences (through Grant No. DE-FG02-98ER14858 to A.Z.P.) is gratefully acknowledged.

APPENDIX: SERIES EXTRAPOLATIONS

In the interest of completeness we present here brief details of the series extrapolation methods employed. Since the primary aim was to provide only semiquantitative comparisons with our simulation results and because, for $q=18$ and 26, only rather short series are available [48–50], we have *not* employed various more sophisticated techniques that make optimal allowance for corrections to scaling (see [43,59]).

Accordingly, the entries in the last column in Table I (for $q=18$ and 26) were obtained by examining $[L/M]$ Padé approximants to the high-temperature series [49] (in powers of K) for $[\chi_T(T)]^{1/\gamma}$ for the assigned value of γ indicated. The dominant zero of the denominator polynomial of each approximant provides an estimate for $K_c=1/T_c^*$. The values quoted reflect the trends of the rather few near-diagonal approximants available.

The dashed plots for the effective exponents in Figs. 3–5 were obtained by using the high- or low-temperature series expansions for the corresponding quantity $Y(x)$, in powers of $x(\leqslant x_c)$, to derive series for the exponent function

$$E(x)=-[\partial \ln Y(x)/\partial \ln(x_c-x)]. \tag{A1}$$

Of course, an estimate for x_c must be used here: we took $T_c^*=4.5114$, 15.52, and 23.24 for $q=6$, 18, and 26, respectively. These values differ slightly from the values listed in Table I; however, the precise values of T_c at this level have negligible consequences for purposes of graphical accuracy. The $[L/M]$ approximants to the series for $E(x)$ were constructed, defective approximants [43,59] were discarded, and a representative approximant was adopted for each case. Specifically, for $\gamma_{\rm eff}^+$, $\gamma_{\rm eff}^-$, and $\beta_{\rm eff}$ we used [8/8], [7/6], and [9/8] for $q=6$, [3/3], [16/16], and [19/19] for $q=18$, and [2/3], [23/24], and [30/31] for $q=26$, respectively.

To construct the biased approximants depicted in the solid plots in Figs. 3–5, in which the preferred value of the exponent, say ζ, is imposed, we wrote

$$E(x)=\zeta[1+G(x)(x_c-x)^{\theta}], \tag{A2}$$

and, accepting $\theta=0.54$ [61], derived series for the correction-to-scaling amplitudes, $G(x)$. Selecting again from the well-behaved approximants $[L/M]$ to $G(x)$, we chose for $\gamma_{\rm eff}^+$, $\gamma_{\rm eff}^-$, and $\beta_{\rm eff}$ (and displayed in Figs. 3–5) the approximants [8/7], [7/7], and [8/9] for $q=6$, [4/2], [18/17], and [22/21] for $q=18$, and [2/3], [24/24], and [30/31] for $q=26$, respectively.

The resulting approximants for $E(x)$ cannot be considered very sound since a little thought reveals that $G(x)$ should have the confluent singularity structure

$$G(x)=G_c+G_{1-\theta}(x_c-x)^{1-\theta}+G_1(x_c-x)+\cdots, \tag{A3}$$

with $1-\theta<1$. Such a function *cannot* be well represented in the critical region by a direct $[L/M]$ Padé approximant. Better results should be obtainable by using *differential approximants* $[K;L/M]$ (see [59,43]), since these can represent a form such as (A3) *exactly* when the higher order terms entail only the powers $(x_c-x)^{k-\theta}$ and $(x_c-x)^k$ for $k=2,3,\ldots$. For the present purposes, however, this refinement was not worthwhile.

Finally, for the amplitude ratio plots in Fig. 7, we accepted $\gamma=1.239$ and the values of T_c^* specified above, and

then constructed direct Padé approximants for the amplitude functions defined via

$$C(x)=(x_c-x)^{\gamma}Y(x), \tag{A4}$$

for $Y(x)=\chi_2^+$ and χ_2^-. As previously, no allowance is thereby made for confluent correction singularities. Furthermore, the approximants for $C^-(x)$ for $q=18$ and 26 exhibit a rather wide spread in the critical region (owing, primarily, to the relatively short series available). The approximants chosen, [17/17] and [25/24], respectively, represent the average behavior satisfactorily. For $C^+(x)$ the [3/4] and [2/3] approximants proved adequate for $q=18$ and 26, respectively.

[1] K. Binder, Ferroelectrics **73**, 43 (1987); Rep. Prog. Phys. **50**, 783 (1987).

[2] *Finite Size Scaling and Numerical Simulations of Statistical Systems*, edited by V. Privman (World Scientific, Singapore, 1990).

[3] *The Monte Carlo Method in Condensed Matter Physics*, edited by K. Binder (Springer-Verlag, Berlin, 1992).

[4] A. M. Ferrenberg and D. P. Landau, Phys. Rev. B **44**, 5081 (1991).

[5] K. Chen, A. M. Ferrenberg, and D. P. Landau, J. Appl. Phys. **73**, 5488 (1993); Phys. Rev. B **48**, 3249 (1993).

[6] H. W. J. Blöte, E. Luijten, and J. R. Heringa, J. Phys. A **28**, 6289 (1995); A. L. Talapov and H. W. J. Blöte, *ibid.* **29**, 5727 (1996).

[7] A. D. Bruce and N. B. Wilding, Phys. Rev. Lett. **68**, 193 (1992); N. B. Wilding and A. D. Bruce, J. Phys.: Condens. Matter **4**, 3087 (1992).

[8] N. B. Wilding, J. Phys.: Condens. Matter **9**, 585 (1997).

[9] K. Binder, Rep. Prog. Phys. **60**, 487 (1997).

[10] P. Seglar and M. E. Fisher, J. Phys. C **13**, 6613 (1980); M. E. Fisher, Phys. Rev. Lett. **57**, 1911 (1986).

[11] K. Binder and H.-P. Deutsch, Europhys. Lett. **18**, 667 (1992).

[12] E. Luijten, H. W. J. Blöte, and K. Binder, Phys. Rev. E **54**, 4626 (1996); Phys. Rev. Lett. **79**, 561 (1997); Phys. Rev. E **56**, 6540 (1997).

[13] E. Luijten and H. W. J. Blöte, Phys. Rev. B **56**, 8945 (1997).

[14] E. Luijten, Phys. Rev. E **59**, 4997 (1999).

[15] M. A. Anisimov, E. Luijten, V. A. Agayan, J. V. Sengers, and K. Binder, Phys. Lett. A **264**, 63 (1999).

[16] E. Luijten and K. Binder, Europhys. Lett. **47**, 311 (1999).

[17] M. A. Anisimov, A. A. Povodyrev, V. D. Kulikov, and J. V. Sengers, Phys. Rev. Lett. **75**, 3146 (1995).

[18] A. A. Povodyrev, M. A. Anisimov, J. V. Sengers, and J. M. H. Levelt Sengers, Physica A **244**, 298 (1997).

[19] Y. B. Melnichenko, M. A. Anisimov, A. A. Povodyrev, G. D. Wignall, J. V. Sengers, and W. A. Van Hook, Phys. Rev. Lett. **79**, 5266 (1997).

[20] See, e.g., M. E. Fisher, Rev. Mod. Phys. **46**, 597 (1974); in *Critical Phenomena*, edited by F. J. W. Hahne, Lecture Notes in Physics Vol. 186 (Springer-Verlag, Berlin, 1983), p. 1.

[21] H. E. Stanley, in *Phase Transitions and Critical Phenomana*, edited by C. Domb and M. S. Green (Academic, London, 1974), Vol. 3, Chap. 7.

[22] L. Vega, E. de Miguel, L. F. Rull, G. Jackson, and I. A. McLure, J. Chem. Phys. **96**, 2296 (1992), and references therein.

[23] E. de Miguel, Phys. Rev. E **55**, 1347 (1997).

[24] J. M. Caillol, D. Levesque, and J. J. Weis, Phys. Rev. Lett. **77**, 4039 (1996); J. Chem. Phys. **107**, 1565 (1997).

[25] J. P. Valleau and G. Torrie, J. Chem. Phys. **108**, 5169 (1998).

[26] G. Orkoulas and A. Z. Panagiotopoulos, J. Chem. Phys. **110**, 1581 (1999).

[27] S.-N. Lai and M. E. Fisher, Mol. Phys. **88**, 1373 (1996) and references therein.

[28] R. R. Singh and K. S. Pitzer, J. Chem. Phys. **92**, 6775 (1990); K. S. Pitzer, Acc. Chem. Res. **23**, 333 (1990).

[29] T. Naraynan and K. S. Pitzer, Phys. Rev. Lett. **73**, 3002 (1994); J. Chem. Phys. **102**, 8118 (1995).

[30] M. L. Japas and J. M. H. Levelt Sengers, J. Phys. Chem. **94**, 5361 (1990).

[31] K. C. Zhang, M. E. Briggs, R. W. Gammon, and J. M. H. Levelt Sengers, J. Chem. Phys. **97**, 8692 (1992); J. M. H. Levelt Sengers and J. A. Given, Mol. Phys. **80**, 899 (1993).

[32] M. Kleemeier, S. Wiegand, W. Schröer, and H. Weingärtner, J. Chem. Phys. **110**, 3085 (1999).

[33] G. Stell, Phys. Rev. A **45**, 7628 (1992).

[34] M. E. Fisher and Y. Levin, Phys. Rev. Lett. **71**, 3826 (1993); J. Stat. Phys. **75**, 1 (1994); J. Phys.: Condens. Matter **8**, 9103 (1996).

[35] G. Stell, J. Stat. Phys. **78**, 197 (1995); J. Phys.: Condens. Matter **8**, 9329 (1996).

[36] B. P. Lee and M. E. Fisher, Phys. Rev. Lett. **76**, 2906 (1996); M. E. Fisher and B. P. Lee, *ibid.* **77**, 3561 (1996).

[37] G. Stell, in *New Approaches to Problems in Liquid State Theory*, edited by C. Caccamo, J.-P. Hansen, and G. Stell, NATO Science Series C Vol. 529 (Kluwer Academic, Dordrecht, 1999), p. 71.

[38] A. G. Moreira, M. M. Telo da Gama, and M. E. Fisher, J. Chem. Phys. **110**, 10 058 (1999).

[39] See, e.g., R. van Roij, M. Dijkstra, and J.-P. Hansen, Phys. Rev. E **59**, 2010 (1999); D. Goulding and J.-P. Hansen, in *New Approaches to Problems in Liquid State Theory* (Ref. [37]), p. 321.

[40] C. Domb, Adv. Phys. **9**, 149 (1960).

[41] C. Domb and M. F. Sykes, J. Math. Phys. **2**, 63 (1961).

[42] M. E. Fisher, Rocky Mt. J. Math. **4**, 181 (1974).

[43] A. J. Guttmann, in *Phase Transitions and Critical Phenomena*, edited by C. Domb and J. L. Lebowitz (Academic, London, 1989), Vol. 13, p. 1.

[44] R. H. Swendsen and J.-S. Wang, Phys. Rev. Lett. **58**, 86 (1987).

[45] U. Wolff, Phys. Rev. Lett. **60**, 1461 (1988); **62**, 361 (1989).

[46] M. E. Fisher, in *Critical Phenomena*, edited by M. S. Green (Academic, New York, 1971), Sec. V, p. 1.

[47] M. E. Fisher and M. N. Barber, Phys. Rev. Lett. **28**, 1516 (1972).

[48] N. W. Dalton, Proc. Phys. Soc. London **88**, 659 (1966).

[49] C. Domb and N. W. Dalton, Proc. Phys. Soc. London **89**, 859 (1966).

[50] N. W. Dalton and D. W. Wood, J. Math. Phys. **10**, 1271 (1969).

[51] D. J. Thouless, Phys. Rev. **181**, 954 (1969).
[52] J. L. Lebowitz and O. Penrose, J. Math. Phys. **7**, 98 (1966).
[53] See, e.g., C. J. Thompson, *Mathematical Statistical Mechanics* (Macmillan, New York, 1972), Secs. 4.4, 4.5, Appendix C.
[54] N. Metropolis, A. W. Rosenbluth, M. N. Rosenbluth, A. H. Teller, and E. Teller, J. Chem. Phys. **21**, 1087 (1953).
[55] A. M. Ferrenberg and R. H. Swendsen, Phys. Rev. Lett. **61**, 2635 (1988); **63**, 1195 (1989).
[56] R. Guida and J. Zinn-Justin, J. Phys. A **31**, 8103 (1998).
[57] See the reviews, Refs. [1–3] and especially the more recent report [9] and references therein.
[58] K. Binder, Z. Phys. B **43**, 119 (1981).
[59] A. J. Liu and M. E. Fisher, Physica A **156**, 35 (1989).
[60] A. J. Liu and M. E. Fisher, J. Stat. Phys. **58**, 431 (1990).
[61] J.-H. Chen, M. E. Fisher, and B. J. Nickel, Phys. Rev. Lett. **48**, 630 (1982).
[62] V. Privman, P. C. Hohenberg, and A. Aharony, in *Phase Transitions and Critical Phenomena*, edited by C. Domb and J. L. Lebowitz (Academic, London, 1991), Vol. 14, p. 1.
[63] S.-Y. Zinn, S.-N. Lai, and M. E. Fisher, Phys. Rev. E **54**, 1176 (1996).
[64] M. E. Fisher and S.-Y. Zinn, J. Phys. A **31**, L629 (1998).
[65] M. Caselle and M. Hasenbusch, J. Phys. A **30**, 4963 (1997).